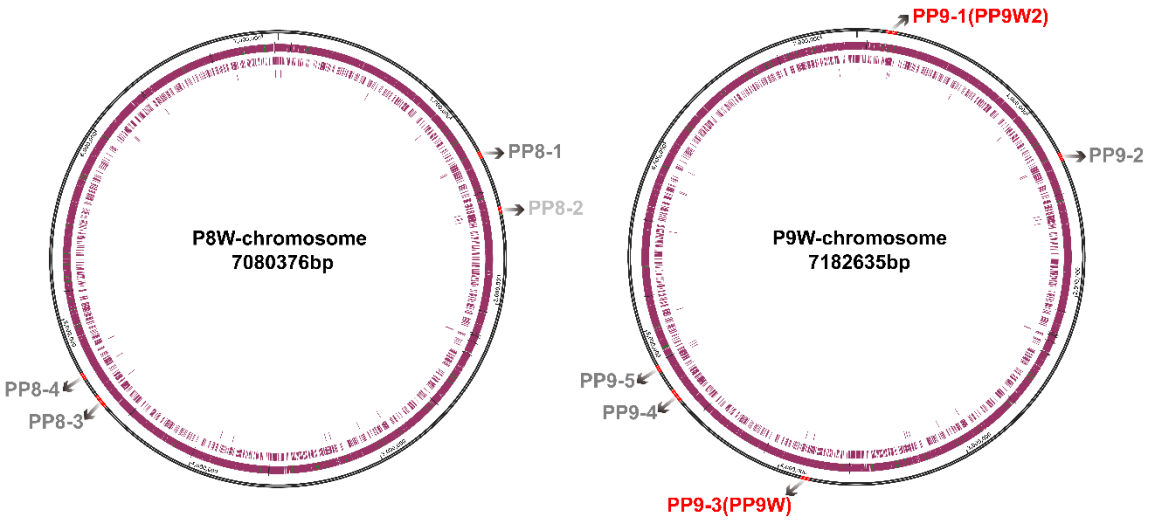

Peophage	Start(bp)	End(bp)	Length(bp)	Category	Score	Closest phage
PP8-1	1212158	1254891	42734	Active	0.95	Pseudomonas phage JBD68
PP8-2	1507710	1543720	36011	Active	0.81	Pseudomonas phage H70
PP8-3	4512609	4584120	71511	Active	0.98	Pseudomonas phage phi2/F10
PP8-4	4680431	4716534	36104	Active	0.83	Pseudomonas phage JD024
PP9W2	148842	203487	54646	Active	0.98	Pseudomonas phage phi1
PP9-2	1253546	1296279	42734	Active	0.95	Pseudomonas phage JBD68
PP9W	3827375	3875417	48043	Active	0.97	Pseudomonas phage phi297
PP9-4	4602431	4673908	71477	Active	0.98	Pseudomonas phage phi2/F10
PP9-5	4779739	4816840	37102	Active	0.95	Pseudomonas phage JD024

Fig S1. The number and location of the predicted active prophages in *P. aeruginosa* P8W and P9W. Upper figure indicates the location of predicted prophages in different genomes. We further identified excised activity of potential active prophages (score > 0.8) in the supernatant of P8W and P9W by plaque PCR using different paired primers listed in Table 2. Only PP9W and PP9W2 (in red) can excised spontaneously. PP8-1/PP9-2, PP8-3/PP9-4 and PP8-4/PP9-5 (in dark grey) were three paired predicted prophages which were highly homologous to each other (>99%). PP8-2 (in light grey) seems to be a specific prophage integrated in P8W, but the corresponding fragment in P9W was indeed highly homologous to it (> 75%).

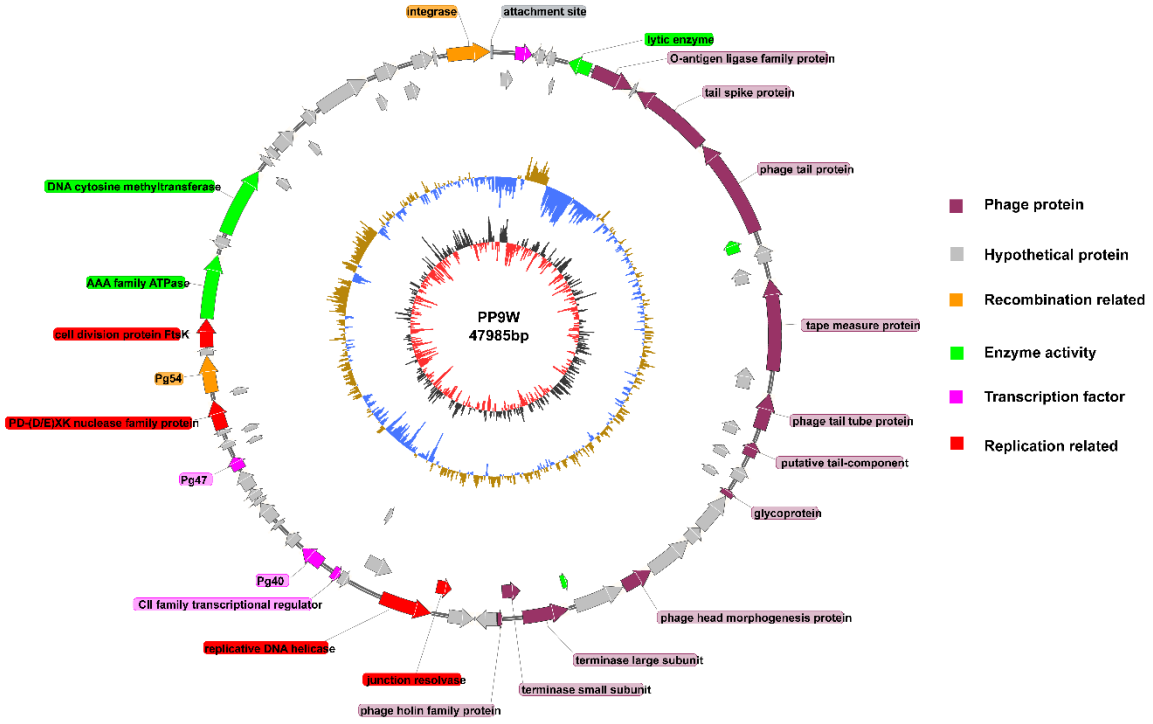

Fig S2. Genome circular map of the *P. aeruginosa* phage PP9W (isolated from the supernatant of P9W). The arrow ring shows the coding sequences (CDS) on the plus and minus strands, respectively. Different colors represent diverse functional proteins. The second ring is GC content. The light yellow part indicates that the GC content in this region is higher than the average GC content in the genome. The higher the peak value is, the greater the difference between the GC content and the average GC content will be. The blue part is on the contrary. The inner ring is GC-skew. Dark gray represents the region where G content is greater than C, and red is opposite. *pg54* encodes the RecT protein (in orange) in this study.

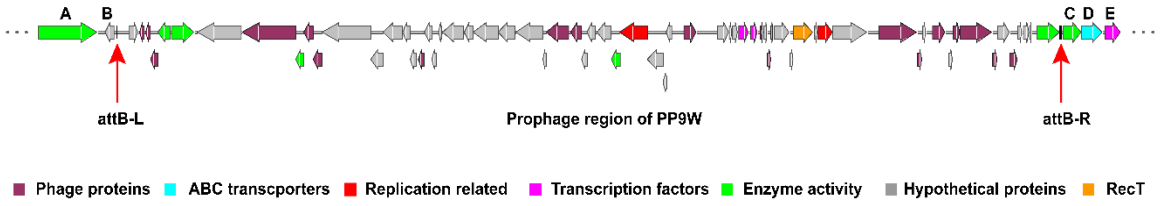

FIG S3 The information on flanking genes from *P. aeruginosa* P9W genome to integrated prophage PP9W. Different colors represent diverse proteins as indicated above. The red arrows show the attachment sites (attB-L and attB-R) of PP9W. A is a putative serine protease; B is a hypothetical protein; C is an Ornithine carbamoyl transferase; D is a ferric iron ABC transporter; E is a UPF0246 protein like YaaA.

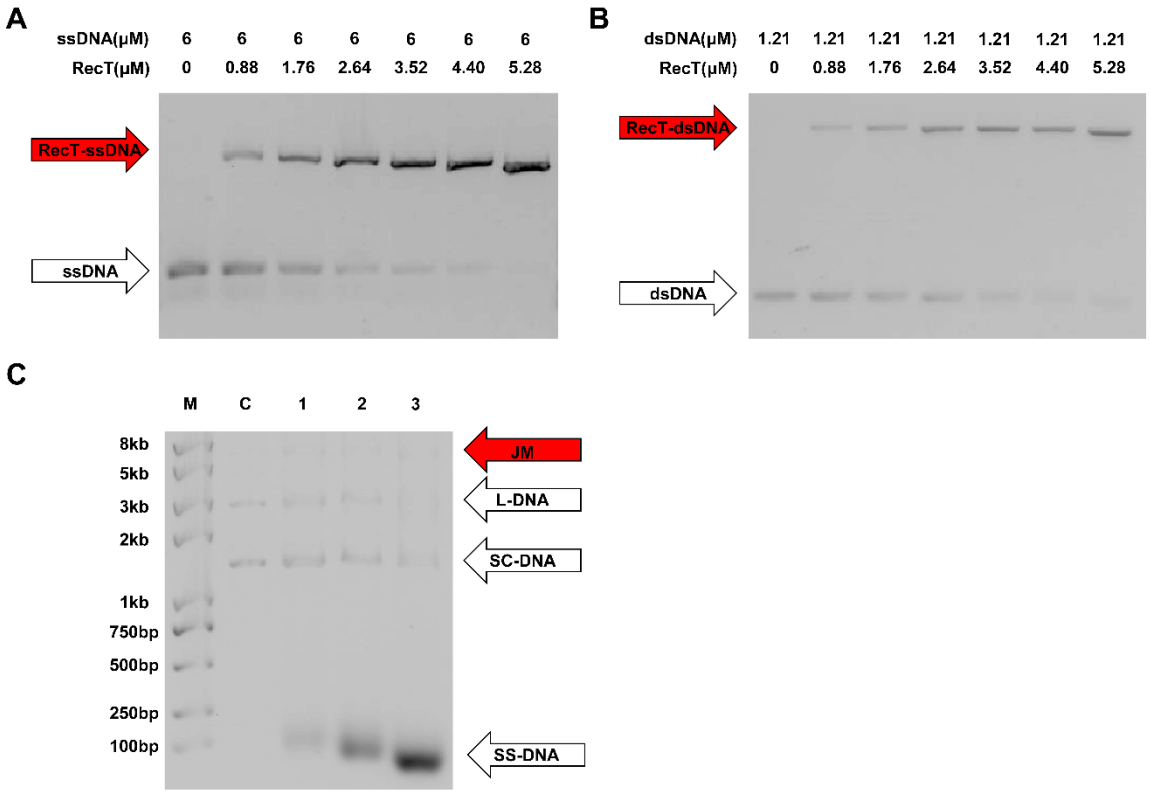

Fig S4. Identification of DNA-binding and strand transfer function of RecT. (A) Electrophoretic mobility shift assay (EMSA) for RecT binding of 50 bp single strand DNA (ssDNA). The red arrow indicates RecT-ssDNA bound complex. The blank arrow indicates free ssDNA. (B) EMSA for RecT binding of 200-300 bp double strand DNA (dsDNA), the promoter region of *pg40*. (C) D-loop formation assay using three different homologous single-stranded oligonucleotide of the plasmid pUC19 (lane 3: 19.1S, lane 4: 19.2S, lane 5: 19.3S, see details in MATERIALS AND METHODS and Table 2). M is DNA marker (lane 1) and C (lane 2) is a control group without addition of ssdNA for initiation of DNA transfer. JM, joint molecules; L-DNA, linear DNA; SC-DNA, supercoil DNA; SS-DNA, free single strand DNA. A black/white inverted image is used here to improve the clarity.

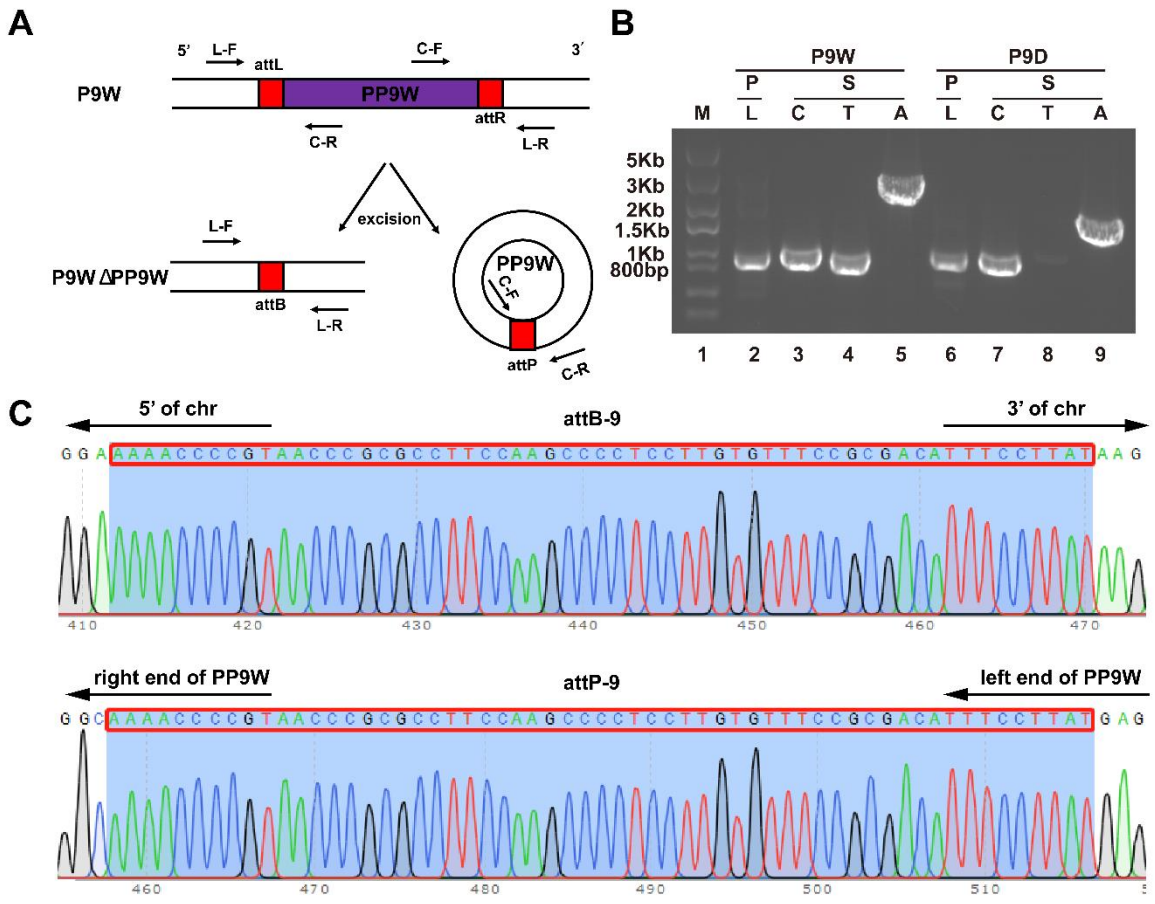

Fig S5. Assay for the excision process. (A) Schematic representation of phage PP9W excision and circularization. Primer pairs L-F/L-R and C-F/C-R are indicated. (B) Detection of PP9W-excised P9W chromosome (lane 2, L: linear form) and the pellet of P9W was used as PCR templates (P). The supernatant of P9W was used as PCR templates for circular form of PP9W (S, lanes 3-5, C: Circular form; T: the amplified fragment contains *recT*; A: the amplified fragment including both upstream and downstream 1Kb of *recT*). P9D related were shown at right (lanes 6-9). (C) PCR products amplifying across the attB-9 and attP-9 sites upon PP9W excision and circularization were sequenced. The 59-bp

attachment site of PP9W is indicated by a red box. 5’ of chr represents 5’ of the chromosome of P9W while 3’ of chr represents 3’ of the chromosome of P9W. Right end of PP9W represents the fragment close to attR while left end of PP9W represents the fragment close to attL indicated by (A, Upper panel). The same results for PP9D condition (data not shown).

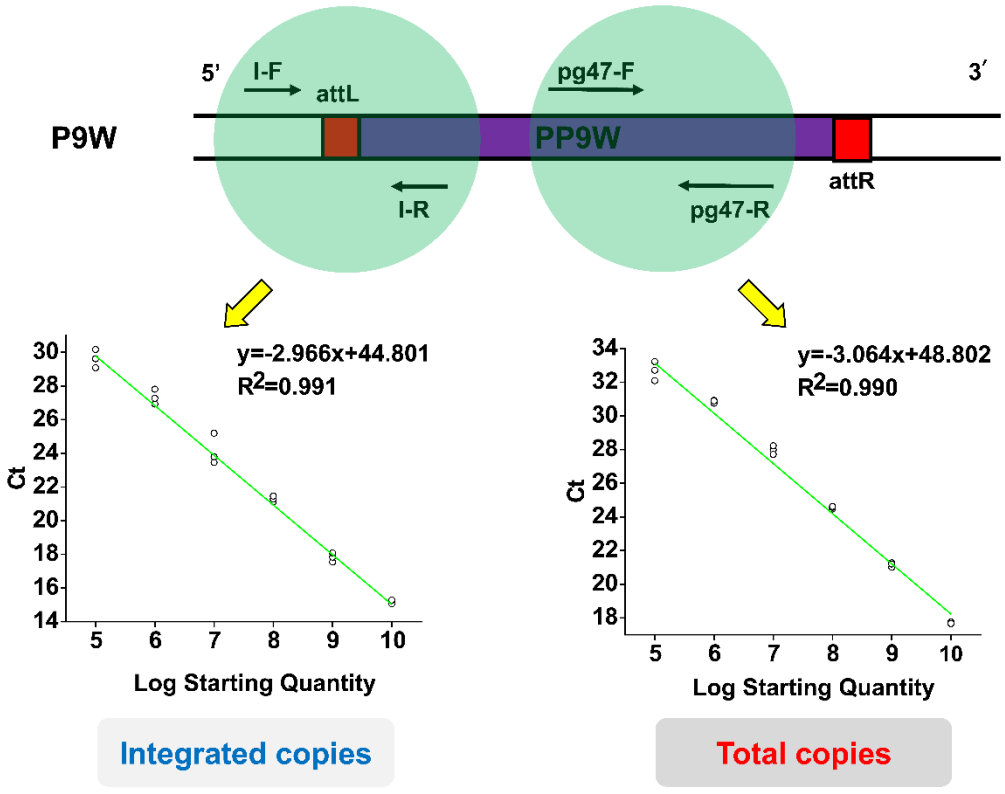

The excision frequency=[(Total copies–Integrated copies)/Total copies] × 100%

Fig S6. Quantitative PCR assay for prophage excision frequency. Integrated PP9W copies was determined using paired primers P9I-F/P9I-R, which amplify a fragment across the attL site only when the prophage is not removed. Total PP9W copies (i.e., integrated + excised) was determined using paired primers pg47-F/pg47-R. The excision frequency was calculated as above. A standard curve was generated for each primer pair using P9W or P9D genomic DNA as PCR templates.

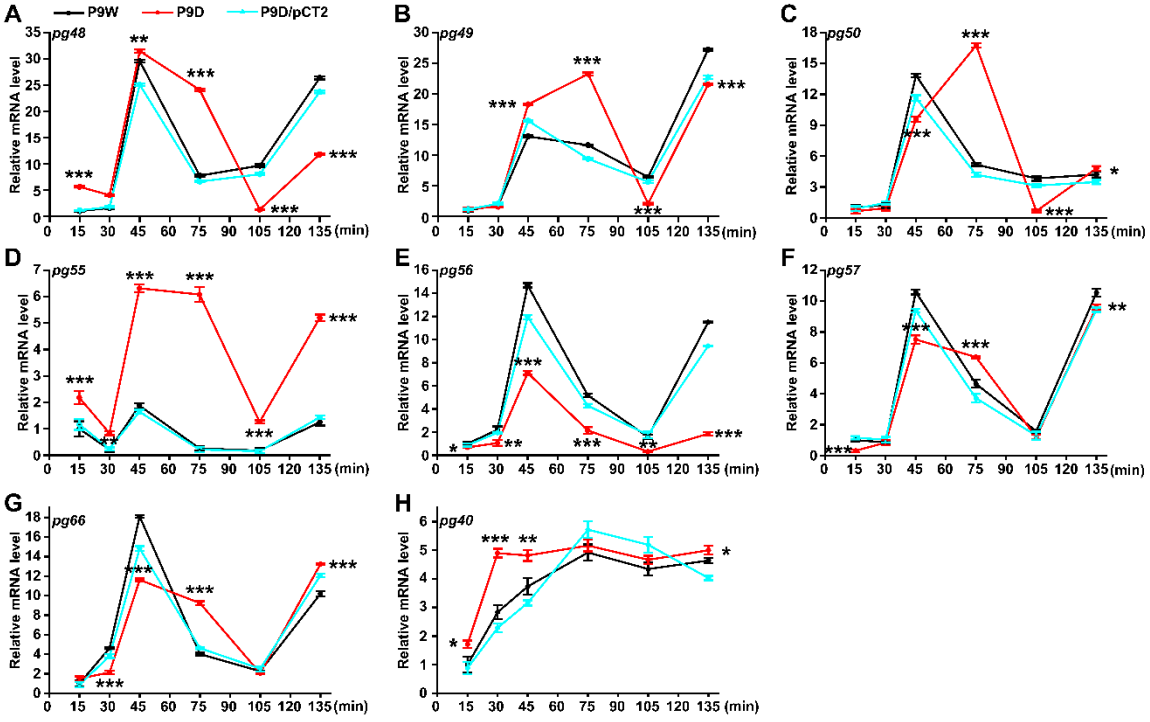

FIG S7 RT-qPCR assay for *recT* related genes (Fig. 2A) expression in the indicated stains. (A-D: *pg48*, *pg49*, *pg50*, *pg55*; G: *pg66*) all encode the hypothetical proteins with gene IDs of PP9W (Fig. 2A). (E) *pg56* encodes a cell division protein. (F) *pg57* encodes a AAA family ATPase. (H) *pg40* encodes a CI-like repressor protein C. The black line indicates the control group and the red line represents the treatment group (r*ecT* deletion). P9D/pCT2 (cyan line) stands for the complementation group. The experiments were independently replicated three times and each sample was tested in triplicate. Error bars show standard deviations. Data were analyzed by one-way analysis of variance (ANOVA) with Tukey's multiple comparisons ($\alpha < 0.05$) to examine the mean differences between the data groups. *, $P < 0.05$. **, $P < 0.01$. ***, $P < 0.001$.

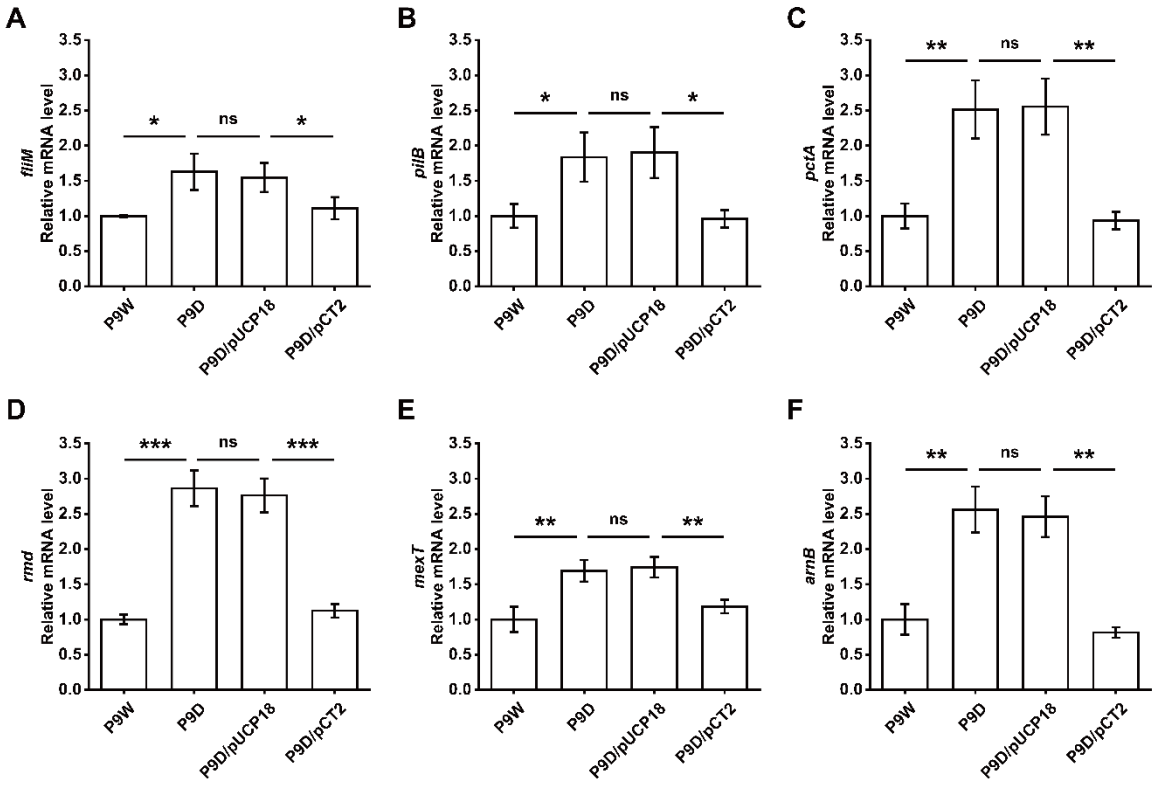

FIG S8 RT-qPCR assay for identification of the transcriptome data. (A) *fliM* encodes a flagellar motor switch protein. (B) *pilB* encodes a type 4 fimbrial biogenesis protein. (C) *pctA* encodes a chemotactic transducer. (D) *rmd* encodes an oxidoreductase. (E) *mexT* encodes a transcriptional regulator. (E) *arnB* encodes an aminotransferase that generates UDP-4-deoxyl-L-arabinose. The experiments were independently replicated three times and each sample was tested in triplicate. Data were analyzed by one-way analysis of variance (ANOVA) with Tukey's multiple comparisons ($\alpha < 0.05$) to examine the mean differences between the data groups. *, $P < 0.05$. **, $P < 0.01$. ***, $P < 0.001$. Error bars show standard deviations.

Table S1. Interactions of 5 clinical *P. aeruginosa* isolates using a spot test.

		Supernatant of test stains				
		P7	P8W	P9W	P18	P27
Indicator strains lawn	P7	-	-	-	-	-
	P8W	+	-	+	-	+
	P9W	-	-	-	-	-
	P18	+	-	+	-	+
	P27	-	-	-	-	-

The vertical columns represent the indicator strains lawn, while the rows show the supernatant of test strains. (+: pairwise strain antagonism shown by zone clearance, -: no evident zone clearance).

Table S2. MIC (minimal inhibitory concentration) of *P. aeruginosa* isolates.

Antibacterial agents[a]	P7	P8W	P9W	P18	P27
Ampicillin	≥32	≥32	≥32	≥32	≥32
Ampicillin/Sulbactam[b]	≥32	≥32	≥32	≥32	≥32
Amikacin	≤2	4	≤2	4	≤2
Aztreonam	≥64	≥64	≥64	≥64	≥64
Ciprofloxacin	≥4	≥4	≥4	≥4	≥4
Cefotetan	≥64	≥64	≥64	≥64	≥64
Ceftriaxone	≥64	≥64	≥64	≥64	≥64
Cefazolin	≥64	≥64	≥64	≥64	≥64
Nitrofurantoin	≥512	≥512	≥512	≥512	≥512
Cefepime	≥64	≥64	≥64	≥64	≥64
Gentamicin	≥16	≥16	≥16	≥16	≥16
Imipenem	≥16	≥16	≥16	≥16	≥16
Levofloxacin	≥8	≥8	≥8	≥8	≥8
Meropenem	≥16	≥16	≥16	≥16	≥16
Piperacillin	≥128	≥128	≥128	≥128	≥128
Cefuroxime-Sodium	≥64	≥64	≥64	≥64	≥64
Cefuroxime-Aaxeril	≥64	≥64	≥64	≥64	≥64
Trimethorprim/Sulfa	≥320	≥320	≥320	≥320	≥320
Ceftazidime	≥64	≥64	≥64	≥64	≥64
Tobramycin	≥16	≥16	≥16	≥16	≥16
Piperacillin/Tazobactam	≥128	≥128	≥128	≥128	≥128

a: MIC unit of the antibiotics used above is μg/mL.

b: A combination of different antibiotics.